Ambiguity Function Analysis for UMTS-Based Passive Multistatic Radar

Sandeep Gogineni, *Member, IEEE*, Muralidhar Rangaswamy, *Fellow, IEEE*, Brian D. Rigling, *Senior Member, IEEE*, and Arye Nehorai, *Fellow, IEEE*

***Abstract*—There has been a growing interest in passive radar systems in the research community over the last decade because of the several merits they offer, including ease of deployment, low cost, and non-detectability of the receivers. During the same period, the idea of distributed MIMO radar and its advantages under the coherent and non-coherent operating scenarios has been extensively studied. Keeping these benefits it mind, in this paper, we consider a UMTS-based passive multistatic radar with distributed antennas. We compute the ambiguity profiles of this radar system under both the coherent and non-coherent modes. The non-coherent processing mode improves the target detection performance by obtaining spatially diverse looks of the target. On the other hand, coherent processing enhances the resolution of target localization. We use numerical examples to demonstrate our analytical results.**

***Index Terms*—Ambiguity function, coherent processing, distributed, multistatic, passive radar, resolution, UMTS signals.**

I. Introduction

THE concept of passive radar systems or passive coherent location systems has been in existence since the 1930s [1]–[3]. This topic has drawn much research attention only during the last decade [4]–[6]. When compared with conventional monostatic systems that have the transmitter and receiver colocated, these systems often rely on signals of opportunity as the transmitted waveforms and the receivers are completely passive and located away from the transmitters [6], [7]. Therefore, the receivers are not detectable and the system to be deployed does not require expensive transmitting hardware. Passive radar systems do not have control over the transmitted waveforms but receive a copy of them directly from the transmitter and this will be used as a reference signal. Signals of opportunity can be from several sources including television [1]–[9] and audio broadcast signals and FM radio [10], [11], satellite-based [12], and mobile communications systems [13].

In this paper, we consider a passive radar system based on universal mobile telecommunications systems (UMTS). These UMTS signals are known to provide high resolution and low sidelobes and hence are of particular interest to the passive radar community. Further, with the rapid increase in their usage globally, the coverage areas for mobile communications systems has increased several-fold in the recent years. Earlier, performance of mobile communications-based passive coherent location systems has been studied using experiments [13] and simulations [14]. More recently, in [15], the authors derived analytical expressions for the monostatic and bistatic ambiguity functions using these UMTS downlink signals. Further, they computed the modified Cramer-Rao lower bound (CRB) for these systems.

Conventional passive radar systems operate in a bistatic configuration. However, very recently, there has been a growing interest in using passive radar systems in multistatic configurations. This is motivated from the several advantages of distributed multiple input multiple output (MIMO) radar systems demonstrated in the last decade [16]–[20]. When operating in a non-coherent configuration [21] these systems exploit spatially diverse looks of the target to improve the detection performance [17]. This goal is accomplished by employing widely spaced transmit and receive antennas. When the target reflections are weak between particular transmitter-receiver pair, it is highly likely that these will be compensated by some of the other pairs that have stronger returns. Further, when there is perfect phase synchronization between all the transmitters and receivers, MIMO radar can operate in a coherent processing mode to enhance the target localization resolution [17], [22]. However, note that when the antennas are too far apart, phase synchronization may not be achievable and in such scenarios, we have to resort to non-coherent processing. It is natural for passive radar systems to benefit from the same reasons by operating in multistatic configuration. In [23], the authors presented a single-stage non-coherent processing approach that performs target detection, localization, and de-ghosting for passive multistatic radar.

In this work, we compute the ambiguity functions for passive multistatic radar systems using UMTS signals (See also [24]). The ambiguity function is an important performance metric for radar systems because it describes the global performance (local accuracy and sidelobes). We consider both the coherent and non-coherent operating scenarios in the Cartesian domain. The delays and Doppler shifts associated with a multistatic system are non-linear functions of the geometry. Therefore, the ambiguity functions are also geometry-dependent. We use numerical examples to study the achievable performance of these sys-

Manuscript received May 25, 2013; revised January 11, 2014; accepted April 11, 2014. Date of publication April 16, 2014; date of current version May 09, 2014. The associate editor coordinating the review of this manuscript and approving it for publication was Dr. Lawrence Carin. M. Rangaswamy was supported by the Air Force Office of Scientific Research under project 2311. A. Nehorai was supported by AFOSR Grant FA9550-11-1-0210.

S. Gogineni is with Wright State Research Institute, Dayton, OH 45435 USA (e-mail: sandeep.gogineni.ctr.in@us.af.mil).

M. Rangaswamy is with Air Force Research Laboratory, Wright Patterson Air Force Base, Dayton OH 45435 USA (e-mail: muralidhar.rangaswamy@us.af.mil).

B. D. Rigling is with the Department of Electrical Engineering, Wright State University, Dayton, OH 45435 USA (e-mail: brian.rigling@wright.edu).

A. Nehorai is with Preston M. Green Department of Electrical and Systems Engineering, Washington University in St. Louis, MO 63130 USA (e-mail: nehorai@ese.wustl.edu).

Color versions of one or more of the figures in this paper are available online at http://ieeexplore.ieee.org.

Digital Object Identifier 10.1109/TSP.2014.2318135

Report Documentation Page

Form Approved
OMB No. 0704-0188

1. REPORT DATE	2. REPORT TYPE	3. DATES COVERED
01 JUN 2014		**00-00-2014 to 00-00-2014**

4. TITLE AND SUBTITLE	5a. CONTRACT NUMBER
Ambiguity Function Analysis for UMTS-Based Passive Multistatic Radar	5b. GRANT NUMBER
	5c. PROGRAM ELEMENT NUMBER
6. AUTHOR(S)	5d. PROJECT NUMBER
	5e. TASK NUMBER
	5f. WORK UNIT NUMBER
7. PERFORMING ORGANIZATION NAME(S) AND ADDRESS(ES) **Wright State Research Institute,Dayton,OH,45435**	8. PERFORMING ORGANIZATION REPORT NUMBER
9. SPONSORING/MONITORING AGENCY NAME(S) AND ADDRESS(ES)	10. SPONSOR/MONITOR'S ACRONYM(S)
	11. SPONSOR/MONITOR'S REPORT NUMBER(S)

12. DISTRIBUTION/AVAILABILITY STATEMENT
Approved for public release; distribution unlimited

13. SUPPLEMENTARY NOTES

14. ABSTRACT

There has been a growing interest in passive radar systems in the research community over the last decade because of the several merits they offer, including ease of deployment low cost, and non-detectability of the receivers. During the same period, the idea of distributed MIMO radar and its advantages under the coherent and non-coherent operating scenarios has been extensively studied. Keeping these benefits it mind, in this paper, we consider a UMTS-based passive multistatic radar with distributed antennas. We compute the ambiguity profiles of this radar system under both the coherent and non-coherent modes. The non-coherent processing mode improves the target detection performance by obtaining spatially diverse looks of the target. On the other hand, coherent processing enhances the resolution of target localization. We use numerical examples to demonstrate our analytical results.

15. SUBJECT TERMS

16. SECURITY CLASSIFICATION OF:			17. LIMITATION OF ABSTRACT	18. NUMBER OF PAGES	19a. NAME OF RESPONSIBLE PERSON
a. REPORT **unclassified**	b. ABSTRACT **unclassified**	c. THIS PAGE **unclassified**	**Same as Report (SAR)**	**13**	

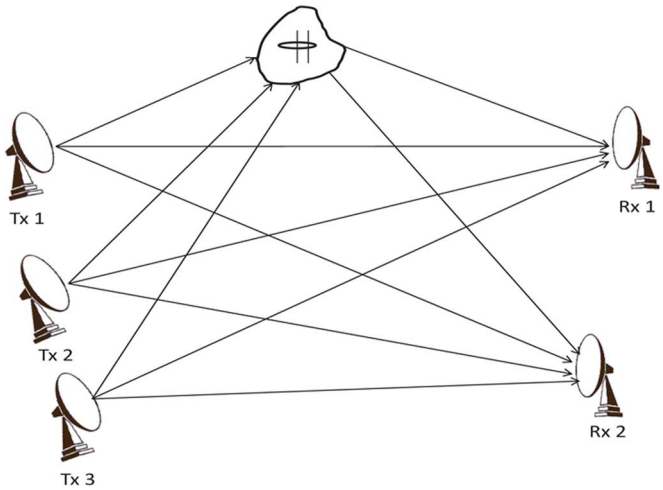

Fig. 1. Passive multistatic radar system (graphic for antennas from [25]).

tems. The rest of the paper is organized as follows. In Section II, we present the transmitted signal model for passive multistatic radar. In Section III, we present the non-coherent measurement model, followed by the detector and the ambiguity function. Similarly, in Section IV, we consider the coherent scenario. In Section V, we present numerical examples of our analytical results. Finally, we provide concluding remarks in Section VI.

II. Signal Model

First, we describe the radar setup in this section, followed by the target models under both the non-coherent and coherent operating modes in the following sections. We consider a passive multistatic radar system consisting of M_{T} transmitters and M_{R} receivers that are widely separated (see Fig. 1). We assume that there is always a line-of-sight component between all transmitter-receiver pairs. In Fig. 1, we have also marked the illuminated scene of interest, the reference paths and the target echo paths for a multistatic system with 3 transmitters and 2 receivers. Let the ith transmitter be located at $\overrightarrow{\boldsymbol{t}_i} = [t_{xi}, t_{yi}, t_{zi}]$. Similarly, the jth receiver is located at $\overrightarrow{\boldsymbol{r}_j} = [r_{xj}, r_{yj}, r_{zj}]$. We assume the transmitters and receivers are stationary but the results can be easily extended to the scenario when they are moving.

We represent the target location and velocity as

$$\overrightarrow{\boldsymbol{p}} = [p_x, p_y, p_z], \tag{1}$$

$$\overrightarrow{\boldsymbol{v}} = [v_x, v_y, v_z]. \tag{2}$$

Therefore, we can define the target state vector

$$\mu = [p_x, p_y, p_z, v_x, v_y, v_z]. \tag{3}$$

Under this set up, the direct or reference path delay between the ith transmitter and the jth receiver is

$$\tau_{ij}^{\mathrm{d}} = \frac{1}{c} \| \overrightarrow{\boldsymbol{t}_i} - \overrightarrow{\boldsymbol{r}_j} \|. \tag{4}$$

Similarly, the delay and Doppler corresponding to the target echo path between the same transceiver pair can be given as [26]

$$\tau_{ij}^{\mu} = \frac{1}{c} \left(\| \overrightarrow{\boldsymbol{p}} - \overrightarrow{\boldsymbol{t}_i} \| + \| \overrightarrow{\boldsymbol{p}} - \overrightarrow{\boldsymbol{r}_j} \| \right), \tag{5}$$

$$f_{\mathrm{D}_{ij}}^{\mu} = \frac{f_{\mathrm{c}}}{c} \left(\langle \overrightarrow{\boldsymbol{v}}, \overrightarrow{\boldsymbol{u}}_{\boldsymbol{r}_j} \rangle - \langle \overrightarrow{\boldsymbol{v}}, \overrightarrow{\boldsymbol{u}}_{\boldsymbol{t}_i} \rangle \right), \tag{6}$$

where c denotes the speed of wave propagation in the medium and f_{c} denotes the carrier frequency; $\overrightarrow{\boldsymbol{u}}_{\boldsymbol{t}_i}$, $\overrightarrow{\boldsymbol{u}}_{\boldsymbol{r}_j}$ denote the unit vector from the ith transmitter to the target and the unit vector from the target to the jth receiver, respectively; $\|.\|$ represents the ℓ_2 norm; and $\langle , \rangle$ is the inner product operator. Clearly, the dependence of the delays and Doppler shifts on the multistatic geometry is non-linear in nature.

As in [15], we consider downlink UMTS signals as our illuminators of opportunity. Let $u_i(t)$ denote the baseband signal corresponding to the ith transmitter. Then

$$u_i(t) = \frac{1}{\sqrt{N}} \sum_{n=0}^{N-1} c_{in} g_i(t - nT), \tag{7}$$

where c_{in} are the transmitted quadrature phase shift keying (QPSK) symbols from the ith transmitter. N is the number of symbols and T is the inverse of the chip rate. All the QPSK symbols are independent and identically distributed across both the transmitter and symbol indices.

$$E\{c_{in} c_{i'n'}\} = \begin{cases} 1, & i = i', n = n'; \\ 0, & \text{otherwise.} \end{cases} \tag{8}$$

The pulse $g_i(t)$ is defined as delayed root-raised-cosine (RRC) pulse $g_i(t) = h_i\left(t - \frac{D}{2}\right)$, where the delay D is selected as

$$\int_{-D/2}^{\frac{D}{2}} h_i^2(t) \mathrm{d}t = 0.95.$$

The RRC pulse $h(t)$ is defined as follows

$$h_i(t) = \frac{\sin\left(\left(\frac{\pi t}{T}\right)(1-\alpha_i)\right) + \left(\frac{4\alpha_i t}{T}\right)\cos\left(\left(\frac{\pi t}{T}\right)(1+\alpha_i)\right)}{\left(\frac{\pi t}{\sqrt{T}}\right)\left[1 - \left(\frac{4\alpha_i t}{T}\right)^2\right]},$$

$$h(t=0) = \frac{1}{\sqrt{T}}\left(1 - \alpha_i + \frac{4\alpha_i}{\pi}\right),$$

$$h\left(t = \pm\frac{T}{4\alpha_i}\right) = \frac{\alpha_i}{\sqrt{2T}}\left[\left(1+\frac{2}{\pi}\right)\sin\left(\frac{\pi}{4\alpha_i}\right) + .\left(1-\frac{2}{\pi}\right)\cos\left(\frac{\pi}{4\alpha_i}\right)\right].$$

The roll-off factor α_i lies in the interval [0,1] for all transmitters. Further analysis on the properties for these waveforms for different parametric values are give in [15]. We skip it here because it is not the main focus of our work. We choose $\alpha_i = 0.22$, $T = 0.26$ μs, and $NT = 0.1$ s. These are typical values for UMTS systems. Having presented the transmit signal model and the radar geometry, we now move on to the two different operating scenarios in the following sections.

III. Non-Coherent Processing

A. Measurement Model

Non-coherent processing is useful to fully exploit the spatial diversity gain. Under this operating mode, we assume the target consists of several individual isotropic scatterers, similar to the model in [17]. We assume the target RCS varies with the angle of view and the different antennas are sufficiently spaced

apart to decorrelate these RCS values. In other words, these RCS values are uncorrelated zero-mean complex Gaussian random variables. If the target RCS values corresponding to certain bistatic pairs are weak, it is highly likely that they will be compensated for by other pairs with strong returns. Let the target RCS corresponding to the ith transmitter and the jth receiver be denoted by β_{ij}. Using a narrowband assumption on the waveforms, we can express the received signal at the jth receiver after down conversion from carrier frequency as

$$y_j^{\mu}(t) = \sum_{i=1}^{M_{\mathrm{T}}} \beta_{ij} u_i\left(t-\tau_{ij}^{\mu}\right) e^{j2\pi\left(f_{\mathrm{D}_{ij}}^{\mu}\left(t-\tau_{ij}^{\mu}\right)-f_{\mathrm{c}}\tau_{ij}^{\mu}\right)} + n_{ij}(t).$$

Expressing in terms of the RRC pulses, we have

$$y_j^{\mu}(t) = \sum_{i=1}^{M_{\mathrm{T}}} \frac{\beta_{ij}}{\sqrt{N}} \sum_{n=0}^{N-1} c_{in} h_i\left(t-nT-\frac{D}{2}-\tau_{ij}^{\mu}\right) \times e^{j2\pi\left(f_{\mathrm{D}_{ij}}^{\mu}\left(t-\tau_{ij}^{\mu}\right)-f_{\mathrm{c}}\tau_{ij}^{\mu}\right)} + n_{ij}(t).$$

The reference or direct path signal from the ith transmitter to the jth receiver is given as

$$y_{ij}^{\mathrm{d}}(t) = u_i\left(t-\tau_{ij}^{\mathrm{d}}\right) e^{-j2\pi f_{\mathrm{c}}\tau_{ij}^{\mathrm{d}}} + n_{ij}^{\mathrm{d}}(t).$$

$n_{ij}(t)$ and $n_{ij}^{\mathrm{d}}(t)$ denote the additive noise terms. We assume that all the direct path and echo signals from different transmitters are separable at each receiver. This is a reasonable assumption as the different transmitters in a UMTS system would not interfere with one another by using separate spectral resources. Next, we will describe the target detector for this problem. We will use this detector to compute the ambiguity function expression.

B. Matched Filter Based Detector

Given this measurement model, the matched-filter based detector reduces to computing the non-coherent test statistic (log-likelihood) corresponding to a state vector μ [17], [27]

$$L^{\mu}(\boldsymbol{y}) \propto \sum_{i=1}^{M_{\mathrm{T}}} \sum_{j=1}^{M_{\mathrm{R}}} \left|y_{ij}^{\mu}\right|^2, \tag{9}$$

where

$$y_{ij}^{\mu} = \int y_j^{\mu}(t) {y_{ij}^{\mathrm{d}}}^{*}\left(t-\tau_{ij}^{\mu}+\tau_{ij}^{\mathrm{d}}\right) e^{-j2\pi f_{\mathrm{D}_{ij}}^{\mu} t}\mathrm{d}t.$$

Expressing the reference signal in terms of the transmitted signal, we obtain

$$y_{ij}^{\mu} = \int y_j^{\mu}(t)\left(u_i^{*}\left(t-\tau_{ij}^{\mu}\right) e^{j2\pi f_{\mathrm{c}}\tau_{ij}^{\mathrm{d}}} + \widetilde{n_{ij}}^{\mathrm{d}}(t)\right) e^{-j2\pi f_{\mathrm{D}_{ij}}^{\mu} t}\mathrm{d}t.$$

The noise term

$$\widetilde{n_{ij}}^{\mathrm{d}}(t) = {n_{ij}^{\mathrm{d}}}^{*}\left(t-\tau_{ij}^{\mu}+\tau_{ij}^{\mathrm{d}}\right).$$

Please note that the test statistic does not depend on the phase term $e^{-j2\pi f_{\mathrm{c}}\tau_{ij}^{\mu}}$ and there are no interference terms from the other transmitters. Even $e^{-j2\pi f_{\mathrm{D}_{ij}}^{\mu}\tau_{ij}^{\mu}}$ does not influence the test statistic. Therefore, phase synchronization is not necessary between transmitters and receivers for this detector. Even though matched filter based detector is the most well-known and a simple way to approach this problem, no claims can be made about optimality because the detection problem is no longer a point hypothesis testing due to the noisy nature of the reference signal and instead becomes a composite hypothesis testing problem. Other more complex signal processing approaches like GLRT may be used but again optimality cannot be claimed. However, note than when the signal to noise ratio of the direct path or reference signal is high, asymptotically the matched filter detector does tend towards optimality because the reference signal will tend towards the transmitted signal.

C. Ambiguity Function

We compute the average ambiguity function corresponding to two target states $\mu = [p_x, p_y, p_z, v_x, v_y, v_z]$ and $\mu' = [p_x', p_y', p_z', v_x', v_y', v_z']$ as $A^{\mu\mu'}$ or $A(p_x, p_y, p_z, v_x, v_y, v_z, p_x', p_y', p_z', v_x', v_y', v_z')$. μ denotes the true target state and we are are comparing with the state μ'. The averaging is done over the transmitted QPSK symbols. As we mentioned earlier, these symbols are independent across the transmitter and symbol indices. Using the above detector, we define the average ambiguity function

$$A^{\mu\mu'} = E\left\{\frac{1}{M_{\mathrm{T}}M_{\mathrm{R}}}\sum_{i=1}^{M_{\mathrm{T}}}\sum_{j=1}^{M_{\mathrm{R}}}\left|\phi_{ij}^{\mu\mu'}\right|^2\right\} \tag{10}$$

where

$$\phi_{ij}^{\mu\mu'} = \int_{-\infty}^{\infty} u_i\left(t-\tau_{ij}^{\mu}\right) e^{-j2\pi f_{\mathrm{D}_{ij}}^{\mu} t} u_i^{*}\left(t-\tau_{ij}^{\mu'}\right) e^{j2\pi f_{\mathrm{D}_{ij}}^{\mu'} t}\mathrm{d}t.$$

Substituting the expressions for the transmitted waveforms, we get

$$\phi_{ij}^{\mu\mu'} = \frac{1}{N}\sum_{n=0}^{N-1}\sum_{n'=0}^{N-1}\int_{-\infty}^{\infty} c_{in} h_i\left(t-nT-\frac{D}{2}-\tau_{ij}^{\mu}\right) \times e^{j2\pi f_{\mathrm{D}_{ij}}^{\mu} t} c_{in'}^{*} h_i^{*}\left(t-n'T-\frac{D}{2}-\tau_{ij}^{\mu'}\right) e^{-j2\pi f_{\mathrm{D}_{ij}}^{\mu'} t}\mathrm{d}t.$$

Define $\chi_{h_i}(.)$ as the monostatic ambiguity function corresponding to the individual RRC pulses from the ith illuminator. Using the expressions we derived in the Appendix for $E\{|\phi_{ij}^{\mu\mu'}|^2\}$, we have the average ambiguity function

$$A^{\mu\mu'} = \frac{1}{M_{\mathrm{T}}M_{\mathrm{R}}N^2}\sum_{i=1}^{M_{\mathrm{T}}}\sum_{j=1}^{M_{\mathrm{R}}} \times \left(\left|\frac{\sin\left(\pi NT\Delta f_{\mathrm{D}_{ij}}^{\mu\mu'}\right)}{\sin\left(\pi T\Delta f_{\mathrm{D}_{ij}}^{\mu\mu'}\right)}\right|^2 \left|\chi_{h_i}\left(\Delta\tau_{ij}^{\mu\mu'}, \Delta f_{\mathrm{D}_{ij}}^{\mu\mu'}\right)\right|^2 + \sum_{n\neq 0, n=-N+1}^{N-1}(N-|n|) \times \left|\chi_{h_i}\left(\Delta\tau_{ij}^{\mu\mu'}+nT, \Delta f_{\mathrm{D}_{ij}}^{\mu\mu'}\right)\right|^2\right).$$

The values of $|\chi_{h_i}(\Delta\tau_{ij}^{\mu\mu'}, \Delta f_{\mathrm{D}_{ij}}^{\mu\mu'})|$ can be easily computed using the result on monostatic ambiguity function in [15]. Note that the dependence of bistatic delay and Doppler terms on the

target positions and velocities is non-linear as we observe from the expressions in Section II. Further, the ambiguity function depends on the multistatic geometry of the passive radar system. In other words, an ambiguity function centered around the origin is no longer sufficient to completely assess the performance of our system. There are two parts in the average ambiguity function summation we presented above. While the first part denotes the self-ambiguity of the pulses, the second part denotes the impact of the interaction between the different pulses on the ambiguity function.

From [15], we observe that the monostatic ambiguity functions corresponding to the individual RRC pulses can be expressed as

$$\begin{aligned}\chi_{h_i}&\left(\Delta\tau_{ij}^{\mu\mu'},\Delta f_{\mathrm{D}_{ij}}^{\mu\mu'}\right)\\&=\int_{-\infty}^{\infty}h_i(t)h_i^*\left(t-\Delta\tau_{ij}^{\mu\mu'}\right)e^{-j2\pi\Delta f_{\mathrm{D}_{ij}}^{\mu\mu'}t}\mathrm{d}t,\\&=H_i\left(\Delta f_{\mathrm{D}_{ij}}^{\mu\mu'}\right)\otimes H_i\left(\Delta f_{\mathrm{D}_{ij}}^{\mu\mu'}\right)e^{j2\pi\Delta f_{\mathrm{D}_{ij}}^{\mu\mu'}\Delta\tau_{ij}^{\mu\mu'}},\end{aligned}$$

where $H_i(\Delta f_{\mathrm{D}_{ij}}^{\mu\mu'})$ denotes the Fourier transform of the RRC pulse $h_i(t)$ and $\otimes$ is the convolution operator. Using the above expression, when the delay $\Delta\tau_{ij}^{\mu\mu'}=0$, the term representing the inter pulse interaction becomes

$$\chi_{h_i}\left(nT,\Delta f_{\mathrm{D}_{ij}}^{\mu\mu'}\right)=H_i\left(\Delta f_{\mathrm{D}_{ij}}^{\mu\mu'}\right)\otimes H_i\left(\Delta f_{\mathrm{D}_{ij}}^{\mu\mu'}\right)e^{j2\pi\Delta f_{\mathrm{D}_{ij}}^{\mu\mu'}nT}.$$

Therefore, we compute the zero-Doppler cut for the non-coherent ambiguity function [see the equation at the bottom of the page]. The zero-delay cut of this ambiguity function

$$\begin{aligned}A^{\mu\mu'}&\Big|_{p_x=p'_x,p_y=p'_y,p_z=p'_z}\\&=\frac{1}{M_{\mathrm{T}}M_{\mathrm{R}}N^2}\sum_{i=1}^{M_{\mathrm{T}}}\sum_{j=1}^{M_{\mathrm{R}}}\\&\quad\times\Bigg(\left|\frac{\sin\left(\pi NT\Delta f_{\mathrm{D}_{ij}}^{\mu\mu'}\right)}{\sin\left(\pi T\Delta f_{\mathrm{D}_{ij}}^{\mu\mu'}\right)}\right|^2\left|H_i\left(\Delta f_{\mathrm{D}_{ij}}^{\mu\mu'}\right)\otimes H_i\left(\Delta f_{\mathrm{D}_{ij}}^{\mu\mu'}\right)\right|^2\\&\qquad+\sum_{n\neq0,n=-N+1}^{N-1}(N-|n|)\\&\qquad\times\left|H_i\left(\Delta f_{\mathrm{D}_{ij}}^{\mu\mu'}\right)\otimes H_i\left(\Delta f_{\mathrm{D}_{ij}}^{\mu\mu'}\right)e^{j2\pi\Delta f_{\mathrm{D}_{ij}}^{\mu\mu'}nT}\right|^2\Bigg),\end{aligned}$$

where $|H_i(\Delta f_{\mathrm{D}_{ij}}^{\mu\mu'})\otimes H_i(\Delta f_{\mathrm{D}_{ij}}^{\mu\mu'})|$ is computed in equation (18) of [15]. Using numerical simulations, we will plot the zero-delay and zero-Doppler cuts computed above to study the ambiguity performance, later in the paper.

IV. Coherent Processing

A. Measurement Model

In the non-coherent processing mode presented above, the target induces uncorrelated phase shifts across the different bistatic transmitter-receiver pairs due to the widely separated nature of the antennas. As a result, it is impossible to coherently combine the outputs at the different receivers. Now, we consider a different scenario under which such coherent processing is possible [16]. In this set up, the target consists of a single point scatterer that has an isotropic complex reflectivity denoted by β. This arrangement preserves the phase information across the different bistatic pairs since there is no multiple scatterer interaction. From now on, when we mention to coherent processing, we refer to this target model. Note that perfect synchronization (phase, time, and frequency) to ensure coherent processing is possible only when the antennas are not too far apart. Otherwise, we have to resort to non-coherent processing described in the previous section. In this paper, we are computing the expressions for both these cases.

Under a narrowband assumption, the baseband received signal at the jth receiver

$$\begin{aligned}y_j^{\mu}(t)&=\sum_{i=1}^{M_{\mathrm{T}}}\beta u_i\left(t-\tau_{ij}^{\mu}\right)e^{j2\pi\left(f_{\mathrm{D}_{ij}}^{\mu}\left(t-\tau_{ij}^{\mu}\right)-f_{\mathrm{c}}\tau_{ij}^{\mu}\right)}+n_{ij}(t),\\&=\sum_{i=1}^{M_{\mathrm{T}}}\frac{\beta}{\sqrt{N}}\sum_{n=0}^{N-1}c_{in}h_i\left(t-nT-\frac{D}{2}-\tau_{ij}^{\mu}\right)\\&\quad\times e^{j2\pi\left(f_{\mathrm{D}_{ij}}^{\mu}\left(t-\tau_{ij}^{\mu}\right)-f_{\mathrm{c}}\tau_{ij}^{\mu}\right)}+n_{ij}(t).\end{aligned}$$

The reference path signal y_j^{d} remains the same as in the non-coherent processing mode since the only difference between the two scenarios stems from the target echo

$$y_{ij}^{\mathrm{d}}(t)=u_i\left(t-\tau_{ij}^{\mathrm{d}}\right)e^{-j2\pi f_{\mathrm{c}}\tau_{ij}^{\mathrm{d}}}+n_{ij}^{\mathrm{d}}(t).$$

$$\begin{aligned}A^{\mu\mu'}\Big|_{v_x=v'_x,v_y=v'_y,v_z=v'_z}&=\frac{1}{M_{\mathrm{T}}M_{\mathrm{R}}N^2}\sum_{i=1}^{M_{\mathrm{T}}}\sum_{j=1}^{M_{\mathrm{R}}}\Bigg(N^2\left|\mathrm{sinc}\left(\frac{\Delta\tau_{ij}^{\mu\mu'}}{T}\right)\frac{\cos\left(\frac{\alpha_i\pi\Delta\tau_{ij}^{\mu\mu'}}{T}\right)}{1-\frac{4\alpha_i^2\Delta\tau_{ij}^{\mu\mu'2}}{T^2}}\right|^2+\sum_{n\neq0,n=-N+1}^{N-1}(N-|n|)\\&\quad\times\left|\mathrm{sinc}\left(\frac{\left(\Delta\tau_{ij}^{\mu\mu'}+nT\right)}{T}\right)\times\frac{\cos\left(\frac{\alpha_i\pi\left(\Delta\tau_{ij}^{\mu\mu'}+nT\right)}{T}\right)}{1-\frac{4\alpha_i^2\left(\Delta\tau_{ij}^{\mu\mu'}+nT\right)^2}{T^2}}\right|^2\Bigg).\end{aligned}$$

B. Matched Filter Based Detector

The coherent test statistic for a matched filter based detector corresponding to the target state μ is given as

$$L^{\mu}(\boldsymbol{y}) \propto \left| \sum_{i=1}^{M_{\mathrm{T}}} \sum_{j=1}^{M_{\mathrm{R}}} y_{ij}^{\mu} \right|^2, \tag{11}$$

where

$$y_{ij}^{\mu} = \int y_j^{\mu}(t) y_{ij}^{\mathrm{d}\,*} \left(t - \tau_{ij}^{\mu} + \tau_{ij}^{\mathrm{d}}\right) \times e^{-j2\pi\left(f_{\mathrm{D}_{ij}}^{\mu}\left(t-\tau_{ij}^{\mu}\right)+f_{\mathrm{c}}\left(\tau_{ij}^{\mu}-\tau_{ij}^{\mathrm{d}}\right)\right)} \mathrm{d}t.$$

We substitute the expression for the reference signal to get

$$y_{ij}^{\mu} = \int y_j^{\mu}(t) \left(u_i^{*}\left(t-\tau_{ij}^{\mu}\right) + \widetilde{n_{ij}^{\mathrm{d}}}(t)\right) \times e^{-j2\pi\left(f_{\mathrm{D}_{ij}}^{\mu}\left(t-\tau_{ij}^{\mu}\right)+f_{\mathrm{c}}\tau_{ij}^{\mu}\right)} \mathrm{d}t,$$

where

$$\widetilde{n_{ij}^{\mathrm{d}}}(t) = n_{ij}^{\mathrm{d}\,*}\left(t-\tau_{ij}^{\mu}+\tau_{ij}^{\mathrm{d}}\right) e^{-j2\pi f_{\mathrm{c}}\tau_{ij}^{\mathrm{d}}}.$$

The dependence of this detector on the phase term is evident from the test statistic.

C. Ambiguity Function

For this case, the ambiguity function must reflect the coherent combination of the different bistatic pair components instead of just combining the amplitudes or energies. Therefore, we define the average coherent ambiguity function as [17], [27]

$$A^{\mu\mu'} = E\left\{ \frac{1}{M_{\mathrm{T}}M_{\mathrm{R}}} \left| \sum_{i=1}^{M_{\mathrm{T}}} \sum_{j=1}^{M_{\mathrm{R}}} \phi_{ij}^{\mu\mu'} \right|^2 \right\} \tag{12}$$

where

$$\phi_{ij}^{\mu\mu'} = \int_{-\infty}^{\infty} u_i\left(t-\tau_{ij}^{\mu}\right) e^{j2\pi f_{\mathrm{D}_{ij}}^{\mu} t} u_i^{*}\left(t-\tau_{ij}^{\mu'}\right) \times e^{-j2\pi f_{\mathrm{D}_{ij}}^{\mu'} t} e^{j2\pi\left(f_{\mathrm{c}}\left(\tau_{ij}^{\mu'}-\tau_{ij}^{\mu}\right)+f_{\mathrm{D_{ij}}}^{\mu'}\tau_{ij}^{\mu'}-f_{\mathrm{D}_{ij}}^{\mu}\tau_{ij}^{\mu}\right)} \mathrm{d}t.$$

After expanding the absolute value of the coherent summation, we can express the average coherent ambiguity function as

$$A^{\mu\mu'} = \frac{1}{M_{\mathrm{T}}M_{\mathrm{R}}} \sum_{i=1}^{M_{\mathrm{T}}} \sum_{j=1}^{M_{\mathrm{R}}} \sum_{i'=1}^{M_{\mathrm{T}}} \sum_{j'=1}^{M_{\mathrm{R}}} E\left\{ \phi_{ij}^{\mu\mu'\,*} \phi_{i'j'}^{\mu\mu'} \right\},$$

Using the derivations we made in the Appendix, we compute the coherent ambiguity function

$$\begin{aligned} &M_{\mathrm{T}}M_{\mathrm{R}}N^2 A^{\mu\mu'} \\ &= \left(\sum_{i=1}^{M_{\mathrm{T}}} \sum_{j=1}^{M_{\mathrm{R}}} \sum_{i'=1}^{M_{\mathrm{T}}} \sum_{j'=1}^{M_{\mathrm{R}}} \right. \\ &\quad \times e^{j2\pi\left(f_{\mathrm{c}}+f_{\mathrm{D}_{i'j'}}^{\mu'}\right)\Delta\tau_{i'j'}^{\mu\mu'}} e^{j2\pi\left(\Delta f_{\mathrm{D}_{ij}}^{\mu\mu'}-\Delta f_{\mathrm{D}_{i'j'}}^{\mu\mu'}\right)\frac{D}{2}} \\ &\quad \times e^{j\pi\left(\Delta f_{\mathrm{D}_{ij}}^{\mu\mu'}-\Delta f_{\mathrm{D}_{i'j'}}^{\mu\mu'}\right)T(N-1)} \chi_{h_i}^{*}\left(\Delta\tau_{ij}^{\mu\mu'}, \Delta f_{\mathrm{D}_{ij}}^{\mu\mu'}\right) \\ &\quad \times \chi_{h_{i'}}\left(\Delta\tau_{i'j'}^{\mu\mu'}, \Delta f_{\mathrm{D}_{i'j'}}^{\mu\mu'}\right) e^{-j2\pi\left(f_{\mathrm{c}}+f_{\mathrm{D_{ij}}}^{\mu'}\right)\Delta\tau_{ij}^{\mu\mu'}} \\ &\quad \left. \times \frac{\sin\left(\pi NT\Delta f_{\mathrm{D}_{ij}}^{\mu\mu'}\right)}{\sin\left(\pi T\Delta f_{\mathrm{D}_{ij}}^{\mu\mu'}\right)} \frac{\sin\left(\pi NT\Delta f_{\mathrm{D}_{i'j'}}^{\mu\mu'}\right)}{\sin\left(\pi T\Delta f_{\mathrm{D}_{i'j'}}^{\mu\mu'}\right)} \right) \\ &\quad + \left(\sum_{i=1}^{M_{\mathrm{T}}} \sum_{j=1}^{M_{\mathrm{R}}} \sum_{j'=1}^{M_{\mathrm{R}}} \sum_{n=0}^{N-1} \sum_{k'\neq n, k'=0}^{N-1} e^{-j2\pi\left(f_{\mathrm{c}}+f_{\mathrm{D_{ij}}}^{\mu'}\right)\Delta\tau_{ij}^{\mu\mu'}} \right. \\ &\quad \times e^{j2\pi\left(f_{\mathrm{c}}+f_{\mathrm{D}_{ij'}}^{\mu'}\right)\Delta\tau_{ij'}^{\mu\mu'}} \\ &\quad \times e^{j2\pi\left(\Delta f_{\mathrm{D}_{ij}}^{\mu\mu'}-\Delta f_{\mathrm{D}_{ij'}}^{\mu\mu'}\right)\frac{D}{2}} e^{j2\pi\left(\Delta f_{\mathrm{D}_{ij}}^{\mu\mu'}-\Delta f_{\mathrm{D}_{ij'}}^{\mu\mu'}\right)nT} \\ &\quad \times \chi_{h_i}^{*}\left(\Delta\tau_{ij}^{\mu\mu'}+(k'-n)T, \Delta f_{\mathrm{D}_{ij}}^{\mu\mu'}\right) \\ &\quad \left. \left. \times \chi_{h_i}\left(\Delta\tau_{ij'}^{\mu\mu'}+(k'-n)T, \Delta f_{\mathrm{D}_{ij'}}^{\mu\mu'}\right) \right) \right). \end{aligned}$$

Using the results in [15], it can be easily verified that the zero-delay cut of the coherent ambiguity function

$$\begin{aligned} &M_{\mathrm{T}}M_{\mathrm{R}}N^2 A^{\mu\mu'}\Big|_{p_x=p'_x, p_y=p'_y, p_z=p'_z} \\ &= \left(\sum_{i=1}^{M_{\mathrm{T}}} \sum_{j=1}^{M_{\mathrm{R}}} \sum_{i'=1}^{M_{\mathrm{T}}} \sum_{j'=1}^{M_{\mathrm{R}}} e^{j2\pi\left(\Delta f_{\mathrm{D}_{ij}}^{\mu\mu'}-\Delta f_{\mathrm{D}_{i'j'}}^{\mu\mu'}\right)\frac{D}{2}} \right. \\ &\quad \times e^{j\pi\left(\Delta f_{\mathrm{D}_{ij}}^{\mu\mu'}-\Delta f_{\mathrm{D}_{i'j'}}^{\mu\mu'}\right)T(N-1)} \\ &\quad \times \left(H_i\left(\Delta f_{\mathrm{D}_{ij}}^{\mu\mu'}\right) \otimes H_i\left(\Delta f_{\mathrm{D}_{ij}}^{\mu\mu'}\right)\right) \\ &\quad \times \left(H_{i'}\left(\Delta f_{\mathrm{D}_{i'j'}}^{\mu\mu'}\right) \otimes H_{i'}\left(\Delta f_{\mathrm{D}_{i'j'}}^{\mu\mu'}\right)\right) \\ &\quad \left. \times \frac{\sin\left(\pi NT\Delta f_{\mathrm{D}_{ij}}^{\mu\mu'}\right)}{\sin\left(\pi T\Delta f_{\mathrm{D}_{ij}}^{\mu\mu'}\right)} \frac{\sin\left(\pi NT\Delta f_{\mathrm{D}_{i'j'}}^{\mu\mu'}\right)}{\sin\left(\pi T\Delta f_{\mathrm{D}_{i'j'}}^{\mu\mu'}\right)} \right) \\ &\quad + \left(\sum_{i=1}^{M_{\mathrm{T}}} \sum_{j=1}^{M_{\mathrm{R}}} \sum_{j'=1}^{M_{\mathrm{R}}} \sum_{n=0}^{N-1} \sum_{k'\neq n, k'=0}^{N-1} e^{j2\pi\left(\Delta f_{\mathrm{D}_{ij}}^{\mu\mu'}-\Delta f_{\mathrm{D}_{ij'}}^{\mu\mu'}\right)\frac{D}{2}} \right. \\ &\quad \times e^{j2\pi\left(\Delta f_{\mathrm{D}_{ij}}^{\mu\mu'}-\Delta f_{\mathrm{D}_{ij'}}^{\mu\mu'}\right)nT} \\ &\quad \times \left(H_i\left(\Delta f_{\mathrm{D}_{ij}}^{\mu\mu'}\right) \otimes H_i\left(\Delta f_{\mathrm{D}_{ij}}^{\mu\mu'}\right) e^{j2\pi\Delta f_{\mathrm{D}_{ij}}^{\mu\mu'}(k'-n)T}\right)^{*} \\ &\quad \left. \left. \times \left(H_i\left(\Delta f_{\mathrm{D}_{ij'}}^{\mu\mu'}\right) \otimes H_i\left(\Delta f_{\mathrm{D}_{ij'}}^{\mu\mu'}\right) e^{j2\pi\Delta f_{\mathrm{D}_{ij'}}^{\mu\mu'}(k'-n)T}\right) \right) \right). \end{aligned}$$

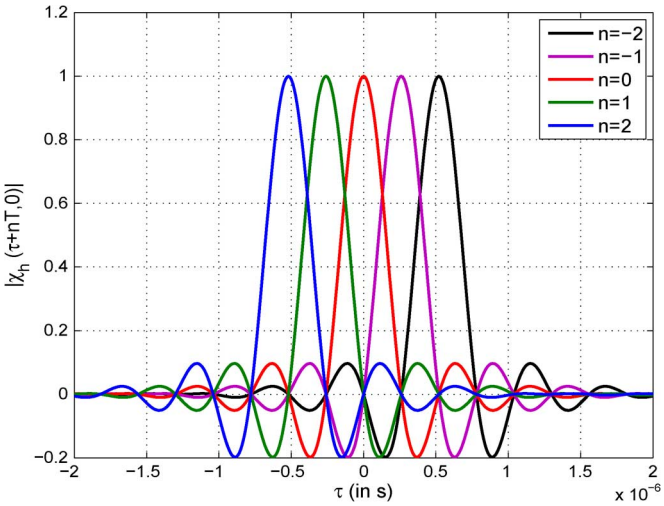

Fig. 2. $|\chi_h(nT+\tau,0)|$ for different n as a function of τ.

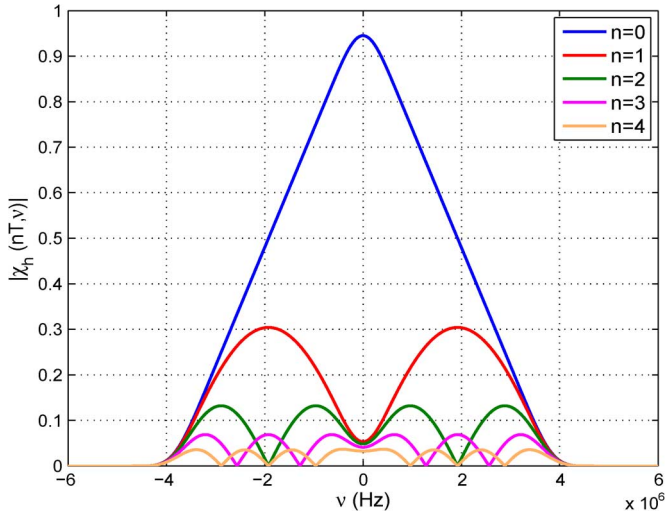

Fig. 3. $|\chi_h(nT,\nu)|$ for different n as a function of ν.

Similarly, the zero-Doppler cut of the coherent-ambiguity function

$$
\begin{aligned}
&M_{\mathrm{T}}M_{\mathrm{R}}N^2A^{\mu\mu'}\Big|_{v_x=v'_x,v_y=v'_y,v_z=v'_z} \\
&= N^2\Bigg(\sum_{i=1}^{M_{\mathrm{T}}}\sum_{j=1}^{M_{\mathrm{R}}}\sum_{i'=1}^{M_{\mathrm{T}}}\sum_{j'=1}^{M_{\mathrm{R}}} e^{-j2\pi\left(f_{\mathrm{c}}+f_{\mathrm{D}_{ij}}^{\mu'}\right)\Delta\tau_{ij}^{\mu\mu'}} \\
&\quad\times e^{j2\pi\left(f_{\mathrm{c}}+f_{\mathrm{D}_{i'j'}}^{\mu'}\right)\Delta\tau_{i'j'}^{\mu\mu'}} \\
&\quad\times \mathrm{sinc}\left(\frac{\Delta\tau_{ij}^{\mu\mu'}}{T}\right)\mathrm{sinc}\left(\frac{\Delta\tau_{i'j'}^{\mu\mu'}}{T}\right) \\
&\quad\times\frac{\cos\left(\frac{\alpha_i\pi\Delta\tau_{ij}^{\mu\mu'}}{T}\right)}{1-\frac{4\alpha_i^2\Delta\tau_{ij}^{\mu\mu'2}}{T^2}}\frac{\cos\left(\frac{\alpha_{i'}\pi\Delta\tau_{i'j'}^{\mu\mu'}}{T}\right)}{1-\frac{4\alpha_{i'}^2\Delta\tau_{i'j'}^{\mu\mu'2}}{T^2}}\Bigg) \\
&+\Bigg(\sum_{i=1}^{M_{\mathrm{T}}}\sum_{j=1}^{M_{\mathrm{R}}}\sum_{j'=1}^{M_{\mathrm{R}}}\sum_{n=0}^{N-1}\sum_{k'\neq n,k'=0}^{N-1} e^{-j2\pi\left(f_{\mathrm{c}}+f_{\mathrm{D}_{ij}}^{\mu'}\right)\Delta\tau_{ij}^{\mu\mu'}} \\
&\quad\times e^{j2\pi\left(f_{\mathrm{c}}+f_{\mathrm{D}_{ij'}}^{\mu'}\right)\Delta\tau_{ij'}^{\mu\mu'}}\mathrm{sinc}\left(\frac{\Delta\tau_{ij}^{\mu\mu'}}{T}+(k'-n)T\right) \\
&\quad\times\mathrm{sinc}\left(\frac{\Delta\tau_{i'j'}^{\mu\mu'}+(k'-n)T}{T}\right) \\
&\quad\times\frac{\cos\left(\frac{\alpha_i\pi\left(\Delta\tau_{ij}^{\mu\mu'}+(k'-n)T\right)}{T}\right)}{1-\frac{4\alpha_i^2\left(\Delta\tau_{ij}^{\mu\mu'}+(k'-n)T\right)^2}{T^2}} \\
&\quad\times\frac{\cos\left(\frac{\alpha_{i'}\pi\left(\Delta\tau_{i'j'}^{\mu\mu'}+(k'-n)T\right)}{T}\right)}{1-\frac{4\alpha_{i'}^2\left(\Delta\tau_{i'j'}^{\mu\mu'}+(k'-n)T\right)^2}{T^2}}\Bigg).
\end{aligned}
$$

Note that unlike the non-coherent scenario, it was not possible to express the average ambiguity function for the coherent case as a summation of just the amplitude-squared terms $|\chi_{h_i}(\Delta\tau_{ij}^{\mu\mu'},\Delta f_{\mathrm{D}_{ij}}^{\mu\mu'})|^2$ due to the presence of the phase terms. Therefore, we expressed in terms of the complex monostatic ambiguity function. The second summation term in the average ambiguity expressions above represents the interaction in between the different pulses of different symbol intervals. Further, even in the coherent case, the ambiguity function depends on the multistatic radar geometry, i.e., the locations of the transmitters, receivers,and the target cell of interest.

V. Numerical Examples

We first examine the impact of the terms denoting the interaction between the pulses in the zero-Doppler and zero-delay cuts, i.e.,

$$
\begin{aligned}
|\chi_h(nT+\tau,0)| &= \left|\mathrm{sinc}\left(\frac{(\tau+nT)}{T}\right)\frac{\cos\left(\frac{\alpha\pi(\tau+nT)}{T}\right)}{1-\frac{4\alpha^2(\tau+nT)^2}{T^2}}\right|, \\
|\chi_h(nT,\nu)| &= \left|H(\nu)\otimes H_i(\nu)e^{j2\pi\nu nT}\right|,
\end{aligned}
$$

for varying n. From Fig. 2, we observe that the cross-terms do have peaks around $\tau=-nT$. This is because at those delays, the two pulses in the ambiguity function from different symbol exactly overlap. However, the scaling factor $\frac{N-|n|}{N^2}$ will attenuate these peaks heavily. Since the integration time for passive radar is typically large, the value of N causes severe attenuation to these cross-pulse peaks making them insignificant in computing the ambiguity function. From Fig. 3, we notice that the impact of the cross-pulse terms is more significant at very high frequencies. However, typical Doppler frequencies are present at the lower end of the spectrum. Around the zero-Doppler point, the contribution of these cross-pulse terms is negligible. This contribution is further attenuated when we multiply by $\frac{N-|n|}{N^2}$. Therefore, we ignore these terms for the simulations.

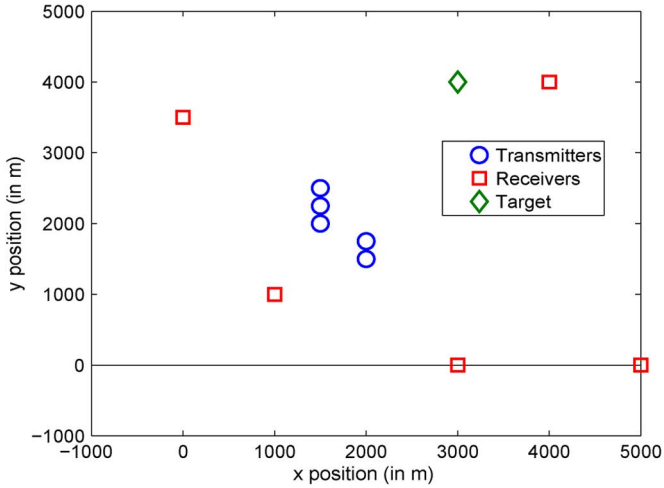

Fig. 4. Simulated multistatic scenario with Transmitter and receiver locations.

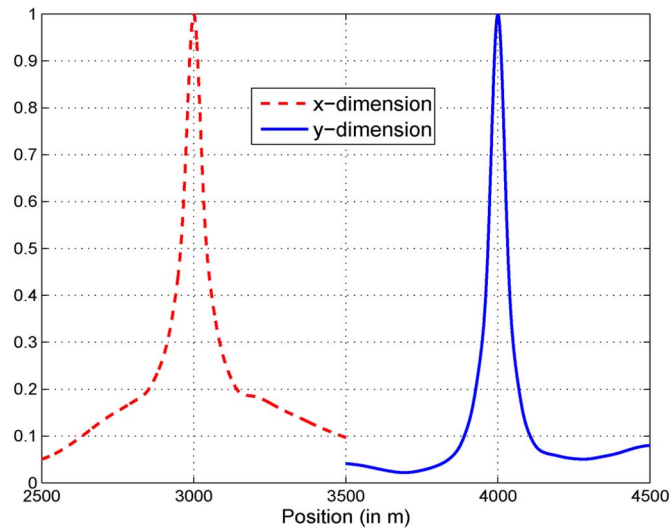

Fig. 6. Non-coherent ambiguity profile in both position dimensions.

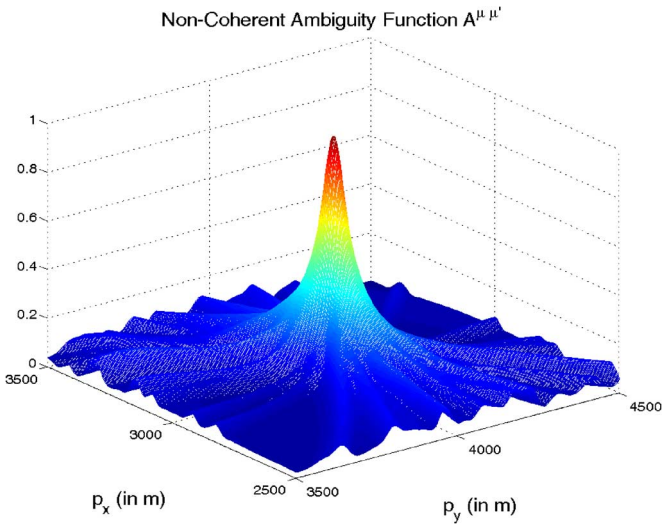

Fig. 5. Zero-Doppler cut of non-coherent ambiguity function when $[p_x, p_y] = [3, 4]$ km and $[v_x, v_y][30, 50]$ m/s.

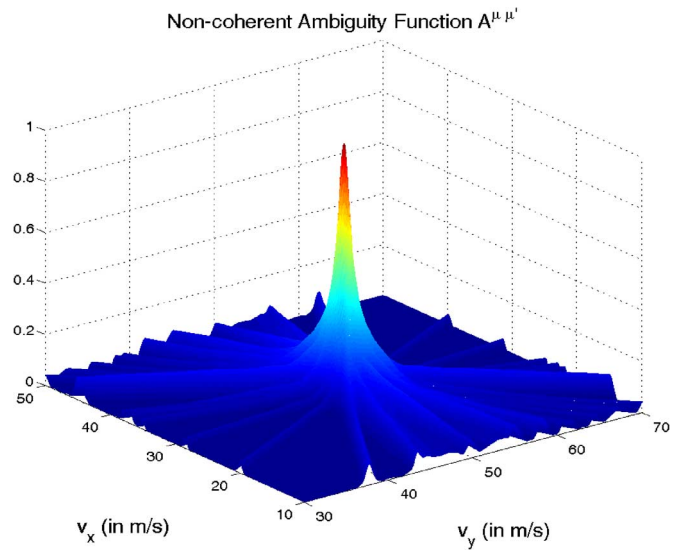

Fig. 7. Zero-delay cut of non-coherent ambiguity function when $[p_x, p_y] = [3, 4]$ km and $[v_x, v_y][30, 50]$ m/s.

We use numerical simulations to demonstrate the ambiguity performance of distributed passive multistatic radar systems. For simplicity, we consider the targets and antennas to be present in the x-y plane but the results will hold true even for the three dimensional case. We consider 5 transmitters and 5 receivers (See Fig. 4) located at

$$\begin{aligned}
\overrightarrow{\boldsymbol{t}_1} &= [0, 2]\ \text{km}; \quad \overrightarrow{\boldsymbol{r}_1} = [3, 0]\ \text{km};\\
\overrightarrow{\boldsymbol{t}_2} &= [0, 3]\ \text{km}; \quad \overrightarrow{\boldsymbol{r}_2} = [5, 0]\ \text{km};\\
\overrightarrow{\boldsymbol{t}_3} &= [0, 5]\ \text{km}; \quad \overrightarrow{\boldsymbol{r}_3} = [0, 3.5]\ \text{km};\\
\overrightarrow{\boldsymbol{t}_4} &= [2, 2]\ \text{km}; \quad \overrightarrow{\boldsymbol{r}_4} = [1, 1]\ \text{km};\\
\overrightarrow{\boldsymbol{t}_5} &= [6, 0]\ \text{km}; \quad \overrightarrow{\boldsymbol{r}_5} = [4, 4]\ \text{km}.
\end{aligned}$$

We compute the ambiguity function in the Cartesian domain centered around the position [3,4] km and velocity [30,50] m/s. We chose the same system parameters as in [15] for the simulations; observation time $NT = 0.1$ s, $T = 0.26$ μs, $\alpha = 0.22$, and the center frequency $f_c = 2100$ MHz.

A. Non-Coherent Processing

First, we begin with the non-coherent operating scenario. In Fig. 5, we plot the zero-Doppler cut of the ambiguity function. We clearly observe that the peak corresponds to the true target position that we are testing. Note that unlike a monostatic or a bistatic configuration, we get a unique peak for the two dimensional ambiguity function instead of a peak circle or ellipse, respectively. Further, when multiple targets are present, multiple peaks corresponding to different targets will be present at the final output of the matched filter processing. In order to observe the resolution in each dimension, we further fix the target location in each dimension to the true value and plot the ambiguity profile in the other dimension (see Fig. 6). We define resolution as the distance between the 20% drop-off points in the main lobe. We observe that the level drops by 20% in the x-dimension at 2850 m and 3150 m. Therefore the position resolution in the x dimension is approximately 300 m. However, in the y-dimension, the level drops below 20% at 3930 m and 4070 m, respectively. Therefore, the resolution is much better in

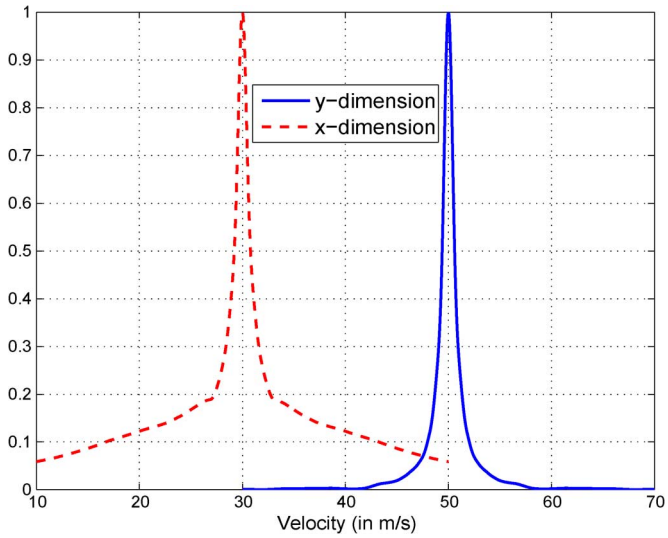

Fig. 8. Non-coherent ambiguity profile in both velocity dimensions.

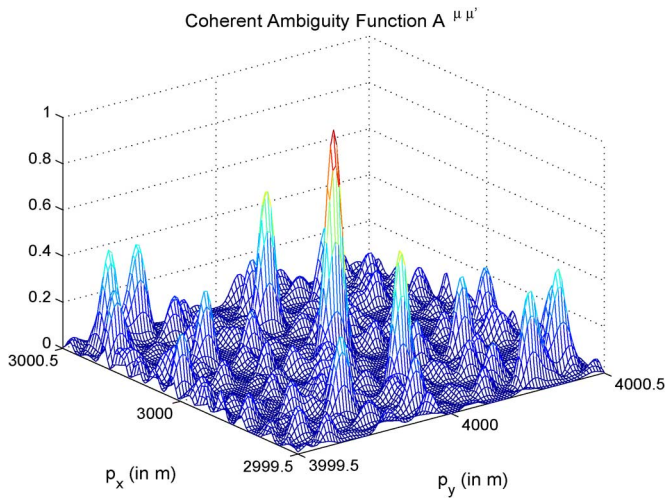

Fig. 9. Zero-Doppler cut of coherent ambiguity function when $[p_x, p_y] = [3, 4]$ km and $[v_x, v_y][30, 50]$ m/s.

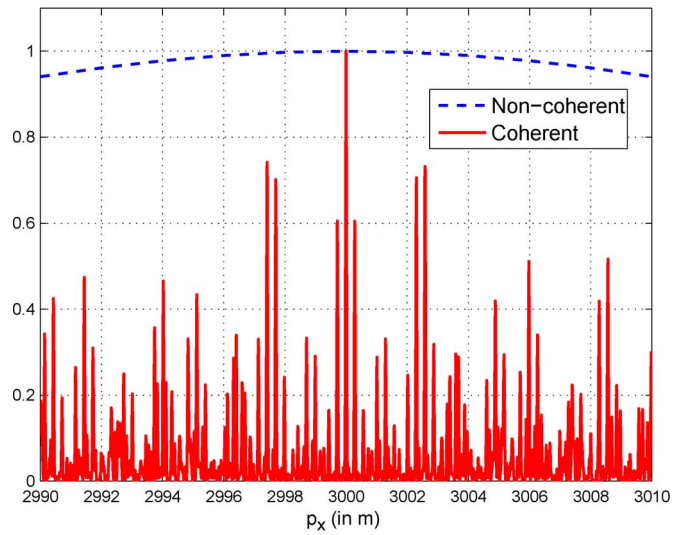

Fig. 10. Coherent and non-coherent ambiguity functions in the x-position dimension.

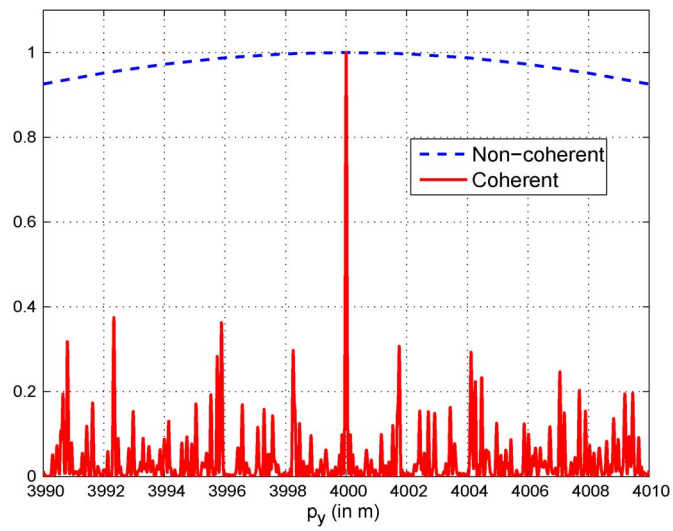

Fig. 11. Coherent and non-coherent ambiguity functions in the y-position dimension.

the y dimension (approximately 140 m). Note that these resolutions depends on the geometry of this specific example and will change depending the locations of the transmitters, receivers, and targets.

Next, we plot the zero-delay cut of the ambiguity function in Fig. 7. The peak corresponds to the true values of the target velocities that we are testing, i.e., [30,50] m/s. Just as we did for the target positions, we fix the target velocity in each dimension and compute the ambiguity profile in the other dimension (see Fig. 8). The velocity resolutions in the x and y dimensions are approximately 5.5 m/s and 2.5 m/s, respectively. Therefore, both the position and velocity resolutions are better in the y dimension for this example.

B. Coherent Processing

Now, we present the coherent-ambiguity function for the same example as the non-coherent case. We expect the additional information in the form of phase will give enhanced resolution performance when compared with non-coherent processing. First, in Fig. 9, we plot the coherent zero-Doppler cut. We notice that the ambiguity function is much sharper when compared with the non-coherent case. Please note that we have zoomed into the ambiguity plot by changing the scales on the x and y axes to capture the exact resolution.

We fix the y-position to the true value and plot the ambiguity function along the x-dimension in Fig. 10. We observe that the resolution for the coherent case is 0.06 m as opposed to 300 m for non-coherent case. We used the same 20% drop-off definition for the resolution. In Fig. 11, we plot the ambiguity functions in the y-dimension. The coherent resolution is 0.1 m compared to 140 m using non-coherent processing. Even though the resolution is slightly poorer in the y-dimension when compared with the x-dimension, we observe that the side-lobes immediately surrounding the main lobe are suppressed to a larger extent in the y-dimension for this example. Note that even though there are significant sidelobes in the coherent processing mode, the peaks of these sidelobes still have a much lower value than the corresponding ambiguity on the mainlobe of the non-coherent processing mode.

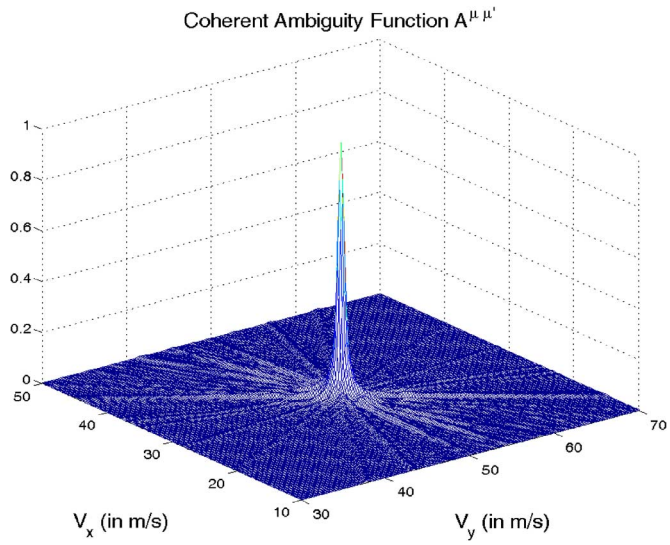

Fig. 12. Zero-delay cut of coherent ambiguity function when $[p_x, p_y] = [3, 4]$ km and $[v_x, v_y][30, 50]$ m/s.

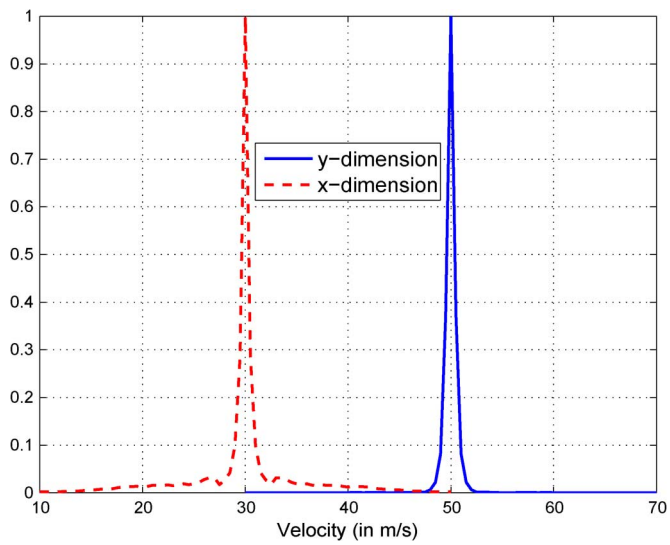

Fig. 13. Coherent ambiguity profile in both velocity dimensions.

Fig. 12 plots the zero-delay cut of the coherent ambiguity function. We observe that the peak coincides with the true target velocity values. In Fig. 13, we plot the coherent ambiguity function in both the velocity dimensions by fixing all the other parameters to the true values. We noticed that the resolutions for the coherent case are approximately 1.5 m/s and 1.6 m/s in the x and y dimensions, respectively. Clearly, the resolution has improved when compared with the non-coherent case.

Note that the coherent and non-coherent ambiguity functions represent the matched filter based detectors under two different target models. Therefore, even though coherent processing offers the enhanced resolution, it is not applicable when the target consists of multiple individual isotropic scatterers, leading to uncorrelated phase shifts across different bistatic pairs. Further, phase synchronization between all the transmitters and receivers is critical for coherent processing and this may not be possible always due to several physical limitations like inaccurate knowledge of the antenna locations and local oscillator characteristics [28]–[30].

VI. Concluding Remarks

We considered a passive distributed radar system using the UMTS downlink as the signals of opportunity. First, we described the multistatic measurement model for this system. Next, we presented the matched filter based detectors under two different operating scenarios; non-coherent and coherent. Then, we computed the ambiguity functions under both these scenarios to analyze the performance. We used numerical examples to demonstrate our analytical results. We observed that passive multistatic radar systems offer sharp resolutions when operating in coherent processing mode.

Since the ambiguity analysis we derived in this paper is geometry-dependent, in future work, we will use these results along with our Cramer-Rao lower bound analysis in [31] to optimally select the illuminators of opportunity from amongst several possible choices. Further, we will extend our analysis beyond UMTS signals to include other classes of illuminators.

Appendix

For the non-coherent processing scenario, we need to compute the amplitude-squared terms

$$\begin{aligned} E\left\{\left|\phi_{ij}^{\mu\mu'}\right|^2\right\} = \frac{1}{N^2}\sum_{n=0}^{N-1}\sum_{n'=0}^{N-1}\sum_{k=0}^{N-1}\sum_{k'=0}^{N-1} E\left\{c_{in}c_{in'}^{*}c_{ik}^{*}c_{ik'}\right\} \\ \times \int_{-\infty}^{\infty}\int_{-\infty}^{\infty} h_i\left(t-nT-\frac{D}{2}-\tau_{ij}^{\mu}\right) e^{j2\pi f_{\mathrm{D}_{ij}}^{\mu} t} \\ \times h_i^{*}\left(t-n'T-\frac{D}{2}-\tau_{ij}^{\mu'}\right) e^{-j2\pi f_{\mathrm{D}_{ij}}^{\mu'} t} \\ \times h_i^{*}\left(t'-kT-\frac{D}{2}-\tau_{ij}^{\mu}\right) e^{-j2\pi f_{\mathrm{D}_{ij}}^{\mu} t'} \\ \times h_i\left(t'-k'T-\frac{D}{2}-\tau_{ij}^{\mu'}\right) e^{j2\pi f_{\mathrm{D}_{ij}}^{\mu'} t'}\,\mathrm{d}t\mathrm{d}t'. \end{aligned}$$

Since the QPSK symbols are independent at different symbol periods,

$$E\left\{c_{in}c_{in'}^{*}c_{ik}^{*}c_{ik'}\right\} = \begin{cases} 1, & n=n',\ k=k'; \\ 1, & n=k,\ n'\neq n,\ n'=k'; \\ 0, & \text{otherwise.} \end{cases}$$

Let $\chi_{h_i}(.)$ denote the monostatic ambiguity function corresponding to the individual RRC pulses from the ith illuminator. The summation can be split into these two conditions as below

$$\begin{aligned} N^2 E\left\{\left|\phi_{ij}^{\mu\mu'}\right|^2\right\} \\ = \left\{\sum_{n=0}^{N-1}\sum_{k=0}^{N-1}\int_{-\infty}^{\infty}\int_{-\infty}^{\infty} h_i\left(t-nT-\frac{D}{2}-\tau_{ij}^{\mu}\right)\right. \\ \times e^{j2\pi f_{\mathrm{D}_{ij}}^{\mu} t} h_i^{*}\left(t-nT-\frac{D}{2}-\tau_{ij}^{\mu'}\right) \\ \times e^{-j2\pi f_{\mathrm{D}_{ij}}^{\mu'} t} h_i^{*}\left(t'-kT-\frac{D}{2}-\tau_{ij}^{\mu}\right) e^{-j2\pi f_{\mathrm{D}_{ij}}^{\mu} t'} \\ \left.\times h_i\left(t'-kT-\frac{D}{2}-\tau_{ij}^{\mu'}\right) e^{j2\pi f_{\mathrm{D}_{ij}}^{\mu'} t'}\,\mathrm{d}t\mathrm{d}t'\right\} \end{aligned}$$

$$+\left\{\sum_{n=0}^{N-1}\sum_{k'\neq n,k'=0}^{N-1}\int_{-\infty}^{\infty}\int_{-\infty}^{\infty} h_i\left(t-nT-\frac{D}{2}-\tau_{ij}^{\mu}\right)\times e^{j2\pi f_{\mathrm{D}_{ij}}^{\mu}t}h_i^*\left(t-k'T-\frac{D}{2}-\tau_{ij}^{\mu'}\right)e^{-j2\pi f_{\mathrm{D}_{ij}}^{\mu'}t}\times h_i^*\left(t'-nT-\frac{D}{2}-\tau_{ij}^{\mu}\right)e^{-j2\pi f_{\mathrm{D}_{ij}}^{\mu}t'}\times h_i\left(t'-k'T-\frac{D}{2}-\tau_{ij}^{\mu'}\right)e^{j2\pi f_{\mathrm{D}_{ij}}^{\mu'}t'}\mathrm{d}t\mathrm{d}t'\right\}.$$

Let

$$\Delta\tau_{ij}^{\mu\mu'}=\tau_{ij}^{\mu'}-\tau_{ij}^{\mu},$$
$$\Delta f_{\mathrm{D}_{ij}}^{\mu\mu'}=f_{\mathrm{D}_{ij}}^{\mu'}-f_{\mathrm{D}_{ij}}^{\mu}.$$

Then,

$$N^2E\left\{\left|\phi_{ij}^{\mu\mu'}\right|^2\right\}=\left|\frac{\sin\left(\pi NT\Delta f_{\mathrm{D}_{ij}}^{\mu\mu'}\right)}{\sin\left(\pi T\Delta f_{\mathrm{D}_{ij}}^{\mu\mu'}\right)}\right|^2\left|\chi_{h_i}\left(\Delta\tau_{ij}^{\mu\mu'},\Delta f_{\mathrm{D}_{ij}}^{\mu\mu'}\right)\right|^2+\sum_{n=0}^{N-1}\sum_{k'\neq n,k'=0}^{N-1}\left|\chi_{h_i}\left(\Delta\tau_{ij}^{\mu\mu'}+(k'-n)T,\Delta f_{\mathrm{D}_{ij}}^{\mu\mu'}\right)\right|^2.$$

Note that the second part of the summation denotes the impact of the interaction between the different pulses on the ambiguity function.

$$N^2E\left\{\left|\phi_{ij}^{\mu\mu'}\right|^2\right\}=\left|\frac{\sin\left(\pi NT\Delta f_{\mathrm{D}_{ij}}^{\mu\mu'}\right)}{\sin\left(\pi T\Delta f_{\mathrm{D}_{ij}}^{\mu\mu'}\right)}\right|^2\left|\chi_{h_i}\left(\Delta\tau_{ij}^{\mu\mu'},\Delta f_{\mathrm{D}_{ij}}^{\mu\mu'}\right)\right|^2+\sum_{n\neq 0,n=-N+1}^{N-1}(N-|n|)\left|\chi_{h_i}\left(\Delta\tau_{ij}^{\mu\mu'}+nT,\Delta f_{\mathrm{D}_{ij}}^{\mu\mu'}\right)\right|^2.$$

For the coherent processing case, instead of the amplitude-squared terms, we need to compute the following terms

$$E\left\{\phi_{ij}^{\mu\mu'*}\phi_{ij'}^{\mu\mu'}\right\}=e^{j\theta_{iji'j'}^{\mu\mu'}}E\left\{\int_{-\infty}^{\infty}u_i^*\left(t-\tau_{ij}^{\mu}\right)e^{-j2\pi f_{\mathrm{D}_{ij}}^{\mu}t}u_i\left(t-\tau_{ij}^{\mu'}\right)\times e^{j2\pi f_{\mathrm{D}_{ij}}^{\mu'}t}\mathrm{d}t\times\int_{-\infty}^{\infty}u_{i'}\left(t'-\tau_{i'j'}^{\mu}\right)\times e^{j2\pi f_{\mathrm{D}_{i'j'}}^{\mu}t'}u_{i'}^*\left(t'-\tau_{i'j'}^{\mu'}\right)e^{-j2\pi f_{\mathrm{D}_{i'j'}}^{\mu'}t'}\mathrm{d}t'\right\},$$

where

$$e^{j\theta_{iji'j'}^{\mu\mu'}}=e^{-j2\pi\left(f_c\Delta\tau_{ij}^{\mu\mu'}+f_{\mathrm{D}_{ij}}^{\mu'}\tau_{ij}^{\mu'}-f_{\mathrm{D}_{ij}}^{\mu}\tau_{ij}^{\mu}\right)}\times e^{j2\pi\left(f_c\Delta\tau_{i'j'}^{\mu\mu'}+f_{\mathrm{D}_{i'j'}}^{\mu'}\tau_{i'j'}^{\mu'}-f_{\mathrm{D}_{i'j'}}^{\mu}\tau_{i'j'}^{\mu}\right)}.$$

Expressing the transmitted waveforms in terms of the individual constituent RRC pulses, we obtain the following

$$E\left\{\phi_{ij}^{\mu\mu'*}\phi_{i'j'}^{\mu\mu'}\right\}=\frac{1}{N^2}\sum_{n=0}^{N-1}\sum_{n'=0}^{N-1}\sum_{k=0}^{N-1}\sum_{k'=0}^{N-1}e^{j\theta_{iji'j'}^{\mu\mu'}}E\left\{c_{in}^*c_{in'}c_{i'k}c_{i'k'}^*\right\}\times\int_{-\infty}^{\infty}\int_{-\infty}^{\infty}h_i^*\left(t-nT-\frac{D}{2}-\tau_{ij}^{\mu}\right)\times h_i\left(t-n'T-\frac{D}{2}-\tau_{ij}^{\mu'}\right)e^{j2\pi\Delta f_{\mathrm{D}_{ij}}^{\mu\mu'}t}\times h_{i'}\left(t'-kT-\frac{D}{2}-\tau_{i'j'}^{\mu}\right)\times h_{i'}^*\left(t'-k'T-\frac{D}{2}-\tau_{i'j'}^{\mu'}\right)e^{-j2\pi\Delta f_{\mathrm{D}_{i'j'}}^{\mu\mu'}t'}\mathrm{d}t\mathrm{d}t'.$$

Since the transmitted QPSK pulses are independent across the different transmitter indices and symbol intervals, we have

$$E\left\{c_{in}^*c_{in'}c_{i'k}c_{i'k'}^*\right\}=\begin{cases}1, & n=n',\ k=k';\\ 1, & n=k,\ n'\neq n,\\ & n'=k',\ i=i';\\ 0, & \text{otherwise.}\end{cases}$$

Substituting the above expression, we obtain

$$N^2E\left\{\phi_{ij}^{\mu\mu'*}\phi_{i'j'}^{\mu\mu'}\right\}=\sum_{n=0}^{N-1}\sum_{k=0}^{N-1}e^{j\theta_{iji'j'}^{\mu\mu'}}\int_{-\infty}^{\infty}\int_{-\infty}^{\infty}h_i^*\left(t-nT-\frac{D}{2}-\tau_{ij}^{\mu}\right)\times h_i\left(t-nT-\frac{D}{2}-\tau_{ij}^{\mu'}\right)e^{j2\pi\Delta f_{\mathrm{D}_{ij}}^{\mu\mu'}t}\times h_{i'}\left(t'-kT-\frac{D}{2}-\tau_{i'j'}^{\mu}\right)\times h_{i'}^*\left(t'-kT-\frac{D}{2}-\tau_{i'j'}^{\mu'}\right)e^{-j2\pi\Delta f_{\mathrm{D}_{i'j'}}^{\mu\mu'}t'}\mathrm{d}t\mathrm{d}t'+\delta_{ii'}\left(\sum_{n=0}^{N-1}\sum_{k'\neq n,k'=0}^{N-1}e^{j\theta_{iji'j'}^{\mu\mu'}}\int_{-\infty}^{\infty}\int_{-\infty}^{\infty}h_i^*\left(t-nT-\frac{D}{2}-\tau_{ij}^{\mu}\right)\times h_i\left(t-k'T-\frac{D}{2}-\tau_{ij}^{\mu'}\right)e^{j2\pi\Delta f_{\mathrm{D}_{ij}}^{\mu\mu'}t}\times h_i\left(t'-nT-\frac{D}{2}-\tau_{ij'}^{\mu}\right)\times h_i^*\left(t'-k'T-\frac{D}{2}-\tau_{ij'}^{\mu'}\right)e^{-j2\pi\Delta f_{\mathrm{D}_{ij'}}^{\mu\mu'}t'}\mathrm{d}t\mathrm{d}t'\right),$$

$$\delta_{ii'} = \begin{cases} 1, & i = i'; \\ 0, & \text{otherwise.} \end{cases}$$

$$N^2 E\left\{\phi_{ij}^{\mu\mu'*}\phi_{i'j'}^{\mu\mu'}\right\} = \left(\sum_{n=0}^{N-1}\sum_{k=0}^{N-1} e^{j\theta_{iji'j'}^{\mu\mu'}}\; e^{j2\pi\left(\Delta f_{\mathrm{D}_{ij}}^{\mu\mu'}\left(\tau_{ij}^{\mu}+nT+\frac{D}{2}\right)-\Delta f_{\mathrm{D}_{i'j'}}^{\mu\mu'}\left(\tau_{i'j'}^{\mu}+kT+\frac{D}{2}\right)\right)}\right.$$
$$\left.\times\chi_{h_i}^{*}\left(\Delta\tau_{ij}^{\mu\mu'},\Delta f_{\mathrm{D}_{ij}}^{\mu\mu'}\right)\chi_{h_{i'}}\left(\Delta\tau_{i'j'}^{\mu\mu'},\Delta f_{\mathrm{D}_{i'j'}}^{\mu\mu'}\right)\right)$$
$$+\delta_{ii'}\left(\sum_{n=0}^{N-1}\sum_{k'\neq n,k'=0}^{N-1} e^{j\theta_{ijij'}^{\mu\mu'}}\; e^{j2\pi\left(\Delta f_{\mathrm{D}_{ij}}^{\mu\mu'}\left(\tau_{ij}^{\mu}+nT+\frac{D}{2}\right)-\Delta f_{\mathrm{D}_{ij'}}^{\mu\mu'}\left(\tau_{ij'}^{\mu}+nT+\frac{D}{2}\right)\right)}\right.$$
$$\left.\times\,\chi_{h_i}^{*}\left(\Delta\tau_{ij}^{\mu\mu'}+(k'-n)T,\Delta f_{\mathrm{D}_{ij}}^{\mu\mu'}\right)\chi_{h_i}\left(\Delta\tau_{ij'}^{\mu\mu'}+(k'-n)T,\Delta f_{\mathrm{D}_{ij'}}^{\mu\mu'}\right)\right).$$

$$N^2 E\left\{\phi_{ij}^{\mu\mu'*}\phi_{i'j'}^{\mu\mu'}\right\} = \left(e^{j\theta_{iji'j'}^{\mu\mu'}}e^{j2\pi\left(\Delta f_{\mathrm{D}_{ij}}^{\mu\mu'}\left(\tau_{ij}^{\mu}+\frac{D}{2}\right)-\Delta f_{\mathrm{D}_{i'j'}}^{\mu\mu'}\left(\tau_{i'j'}^{\mu}+\frac{D}{2}\right)\right)}\;\chi_{h_i}^{*}\left(\Delta\tau_{ij}^{\mu\mu'},\Delta f_{\mathrm{D}_{ij}}^{\mu\mu'}\right)\chi_{h_{i'}}\left(\Delta\tau_{i'j'}^{\mu\mu'},\Delta f_{\mathrm{D}_{i'j'}}^{\mu\mu'}\right)\right.$$
$$\left.\times\sum_{n=0}^{N-1}\sum_{k=0}^{N-1} e^{j2\pi\left(\Delta f_{\mathrm{D}_{ij}}^{\mu\mu'}n-\Delta f_{\mathrm{D}_{i'j'}}^{\mu\mu'}k\right)T}\right)$$
$$+\delta_{ii'}\left(\sum_{n=0}^{N-1}\sum_{k'\neq n,k'=0}^{N-1} e^{j\theta_{ijij'}^{\mu\mu'}}\; e^{j2\pi\left(\Delta f_{\mathrm{D}_{ij}}^{\mu\mu'}\left(\tau_{ij}^{\mu}+nT+\frac{D}{2}\right)-\Delta f_{\mathrm{D}_{ij'}}^{\mu\mu'}\left(\tau_{ij'}^{\mu}+nT+\frac{D}{2}\right)\right)}\right.$$
$$\left.\times\,\chi_{h_i}^{*}\left(\Delta\tau_{ij}^{\mu\mu'}+(k'-n)T,\Delta f_{\mathrm{D}_{ij}}^{\mu\mu'}\right)\chi_{h_i}\left(\Delta\tau_{ij'}^{\mu\mu'}+(k'-n)T,\Delta f_{\mathrm{D}_{ij'}}^{\mu\mu'}\right)\right).$$

---

where [see the equation at the top of the page]. Upon simplification,

$$N^2 E\left\{\phi_{ij}^{\mu\mu'*}\phi_{i'j'}^{\mu\mu'}\right\}$$
$$= \left(e^{j\theta_{iji'j'}^{\mu\mu'}}e^{j2\pi\left(\Delta f_{\mathrm{D}_{ij}}^{\mu\mu'}\left(\tau_{ij}^{\mu}+\frac{D}{2}\right)-\Delta f_{\mathrm{D}_{i'j'}}^{\mu\mu'}\left(\tau_{i'j'}^{\mu}+\frac{D}{2}\right)\right)}\right.$$
$$\times\chi_{h_i}^{*}\left(\Delta\tau_{ij}^{\mu\mu'},\Delta f_{\mathrm{D}_{ij}}^{\mu\mu'}\right)\chi_{h_{i'}}\left(\Delta\tau_{i'j'}^{\mu\mu'},\Delta f_{\mathrm{D}_{i'j'}}^{\mu\mu'}\right)$$
$$\times e^{j\pi\left(\Delta f_{\mathrm{D}_{ij}}^{\mu\mu'}-\Delta f_{\mathrm{D}_{ij'}}^{\mu\mu'}\right)T(N-1)}$$
$$\left.\times\frac{\sin\left(\pi NT\Delta f_{\mathrm{D}_{ij}}^{\mu\mu'}\right)}{\sin\left(\pi T\Delta f_{\mathrm{D}_{ij}}^{\mu\mu'}\right)}\frac{\sin\left(\pi NT\Delta f_{\mathrm{D}_{i'j'}}^{\mu\mu'}\right)}{\sin\left(\pi T\Delta f_{\mathrm{D}_{i'j'}}^{\mu\mu'}\right)}\right)$$
$$+\delta_{ii'}\left(\sum_{n=0}^{N-1}\sum_{k'\neq n,k'=0}^{N-1} e^{j\theta_{ijij'}^{\mu\mu'}}\right.$$
$$\times e^{j2\pi\left(\Delta f_{\mathrm{D}_{ij}}^{\mu\mu'}\left(\tau_{ij}^{\mu}+nT+\frac{D}{2}\right)-\Delta f_{\mathrm{D}_{ij'}}^{\mu\mu'}\left(\tau_{ij'}^{\mu}+nT+\frac{D}{2}\right)\right)}$$
$$\times\chi_{h_i}^{*}\left(\Delta\tau_{ij}^{\mu\mu'}+(k'-n)T,\Delta f_{\mathrm{D}_{ij}}^{\mu\mu'}\right)$$
$$\left.\times\chi_{h_i}\left(\Delta\tau_{ij'}^{\mu\mu'}+(k'-n)T,\Delta f_{\mathrm{D}_{ij'}}^{\mu\mu'}\right)\right),$$

Substituting this expression gives the average ambiguity function $A^{\mu\mu'}$

$$M_{\mathrm{T}}M_{\mathrm{R}}N^2A^{\mu\mu'}$$
$$= \left(\sum_{i=1}^{M_{\mathrm{T}}}\sum_{j=1}^{M_{\mathrm{R}}}\sum_{i'=1}^{M_{\mathrm{T}}}\sum_{j'=1}^{M_{\mathrm{R}}} e^{j\theta_{iji'j'}^{\mu\mu'}}\right.$$
$$\times e^{j2\pi\left(\Delta f_{\mathrm{D}_{ij}}^{\mu\mu'}\left(\tau_{ij}^{\mu}+\frac{D}{2}\right)-\Delta f_{\mathrm{D}_{i'j'}}^{\mu\mu'}\left(\tau_{i'j'}^{\mu}+\frac{D}{2}\right)\right)}$$
$$\times\chi_{h_i}^{*}\left(\Delta\tau_{ij}^{\mu\mu'},\Delta f_{\mathrm{D}_{ij}}^{\mu\mu'}\right)\chi_{h_i'}\left(\Delta\tau_{i'j'}^{\mu\mu'},\Delta f_{\mathrm{D}_{i'j'}}^{\mu\mu'}\right)$$
$$\times e^{j\pi\left(\Delta f_{\mathrm{D}_{ij}}^{\mu\mu'}-\Delta f_{\mathrm{D}_{i'j'}}^{\mu\mu'}\right)T(N-1)}$$
$$\left.\times\frac{\sin\left(\pi NT\Delta f_{\mathrm{D}_{ij}}^{\mu\mu'}\right)}{\sin\left(\pi T\Delta f_{\mathrm{D}_{ij}}^{\mu\mu'}\right)}\frac{\sin\left(\pi NT\Delta f_{\mathrm{D}_{i'j'}}^{\mu\mu'}\right)}{\sin\left(\pi T\Delta f_{\mathrm{D}_{i'j'}}^{\mu\mu'}\right)}\right)$$
$$+\left(\sum_{i=1}^{M_{\mathrm{T}}}\sum_{j=1}^{M_{\mathrm{R}}}\sum_{j'=1}^{M_{\mathrm{R}}}\sum_{n=0}^{N-1}\sum_{k'\neq n,k'=0}^{N-1} e^{j\theta_{ijij'}^{\mu\mu'}}\right.$$
$$\times e^{j2\pi\left(\Delta f_{\mathrm{D}_{ij}}^{\mu\mu'}\left(\tau_{ij}^{\mu}+nT+\frac{D}{2}\right)-\Delta f_{\mathrm{D}_{ij'}}^{\mu\mu'}\left(\tau_{ij'}^{\mu}+nT+\frac{D}{2}\right)\right)}$$
$$\times\chi_{h_i}^{*}\left(\Delta\tau_{ij}^{\mu\mu'}+(k'-n)T,\Delta f_{\mathrm{D}_{ij}}^{\mu\mu'}\right)$$
$$\left.\times\chi_{h_i}\left(\Delta\tau_{ij'}^{\mu\mu'}+(k'-n)T,\Delta f_{\mathrm{D}_{ij'}}^{\mu\mu'}\right)\right).$$

REFERENCES

[1] H. D. Griffiths and N. R. W. Long, "Television based bistatic radar," *IEE Proc. F, Commun. Radar Signal Process.*, vol. 133, pp. 649–657, 1986.

[2] J. M. Hawkins, "An opportunistic bistatic radar," in *Proc. Inst. Electr. Eng. Radar Conf.*, Oct. 1997, pp. 318–322.

[3] M. A. Ringer and G. J. Frazer, "Waveform analysis of transmissions of opportunity for passive radar," in *Proc. 5th Int. Symp. Signal Process. Appl.*, Aug. 1999, pp. 511–514.

[4] H. D. Griffiths and C. J. Baker, "Passive coherent location radar systems. Part 1: Performance prediction," in *Proc. Inst. Electr. Eng.—Radar, Sonar, Navigat.*, 2005, vol. 152, no. 3, pp. 153–159.

[5] C. J. Baker, H. D. Griffiths, and I. Papoutsis, "Passive coherent location radar systems. Part 2: Waveform properties," in *Proc. Inst. Electr. Eng. —Radar, Sonar, Navigat.*, 2005, pp. 160–168.

[6] M. Malanowski and K. Kulpa, "Digital beamforming for passive coherent location radar," presented at the Radar Conf., Rome, Italy, May 2008.

[7] M. Malanowski, "Detection and parameter estimation of manoeuvring targets with passive bistatic radar," *IET Radar Sonar Navigat.*, vol. 6, pp. 739–745, Oct. 2012.

[8] P. E. Howland, "Target tracking using television-based bistatic radar," *Proc. Inst. Electr. Eng.—Radar, Sonar ,Navigat,*, vol. 146, pp. 166–174, Jun. 1999.

[9] H. A. Harms, L. M. Davis, and J. Palmer, "Understanding the signal structure in DVB-T signals for passive radar detection," presented at the IEEE Int. Radar Conf., Washington, DC, USA, May 2010.

[10] A. D. Lallo, A. Farina, R. Fulcoli, P. Genovesi, R. Lalli, and R. Mancinelli, "Design, development and test on real data of an FM based prototypical passive radar," in *Proc. IEEE Radar Conf.*, Rome, Italy, May 2008.

[11] D. Poullin, "Passive detection using digitial broadcasters (DAB, DVB) with COFDM modulation," *Proc. Inst. Electr. Eng.—Radar, Sonar, Navigat.*, vol. 152, Jun. 2005.

[12] H. D. Griffiths, A. J. Garnett, C. J. Baker, and S. Keaveney, "Bistatic radar using satellite-borne illuminators of opportunity," in *Proc. Int. Radar Conf.*, Oct. 1992, pp. 276–279.

[13] H. D. Griffiths and C. J. Baker, "Measurement and analysis of ambiguity functions of passive radar transmissions," presented at the IEEE Int. Radar Conf., Washington, DC, USA, May 2005.

[14] D. Petri, A. Capria, M. Martorella, and F. Berizzi, "Ambiguity function study for UMTS passive radar," presented at the 6th Eur. Radar Conf., Rome, Italy, Sep. 2009.

[15] P. Stinco, M. S. Greco, F. Gini, and M. Rangaswamy, "Ambiguity function and Cramer-rao bounds for universal mobile telecommunications system-based passive coherent location systems," *IET Radar Sonar Navigat.*, vol. 6, pp. 668–678, Aug. 2012.

[16] J. Li and P. Stoica, *MIMO Radar Signal Processing*. Hoboken, NJ, USA: Wiley, 2009.

[17] A. M. Haimovich, R. S. Blum, and L. J. Cimini, "MIMO radar with widely separated antennas," *IEEE Signal Process. Mag.*, vol. 25, pp. 116–129, Jan. 2008.

[18] S. Gogineni and A. Nehorai, "Target estimation using sparse modeling for distributed MIMO radar," *IEEE Trans. Signal Process.*, vol. 59, pp. 5315–5325, Nov. 2011.

[19] H. Godrich, A. M. Haimovich, and R. S. Blum, "Target localization accuracy gain in MIMO radar-based systems," *IEEE Trans. Inf. Theory*, vol. 56, pp. 2783–2803, June 2010.

[20] S. Gogineni and A. Nehorai, "Polarimetric MIMO radar with distributed antennas for target detection," in *Proc. 43rd Asilomar Conf. Signals, Syst., Comput.*, Pacific Grove, CA, USA, Nov. 2009, pp. 1144–1148.

[21] X. Chen and R. Blum, "Non-coherent MIMO radar in a non-Gaussian noise-plus-clutter environment," in *Proc. 44th Annu. Conf. Inf. Sci. Syst. (CISS)*, Princeton, NJ, USA, Mar. 2010, pp. 1–6.

[22] Y. Yang and R. S. Blum, "Phase synchronization for coherent MIMO radar: Algorithms and their analysis," *IEEE Trans. Signal Process.*, vol. 59, pp. 5538–5557, Nov. 2011.

[23] D. E. Hack, L. K. Patton, A. D. Kerrick, and M. A. Saville, "Direct Cartesian detection, localization, and de-ghosting for passive multistatic radar," presented at the 7th IEEE Sensor Array Multichannel Signal Process. Workshop, Hoboken, NJ, USA, Jun. 2012.

[24] S. Gogineni, M. Rangaswamy, B. Rigling, and A. Nehorai, "Ambiguity function analysis for passive multistatic radar using UMTS signals," presented at the IEEE Radar Conf., Cincinnati, OH, USA, May 2014.

[25] National Weather Service: JetStream—Online School for Weather [Online]. Available: http://www.srh.noaa.gov/jetstream/doppler/how.htm

[26] S. Gogineni and A. Nehorai, "Adaptive design for distributed MIMO radar using sparse modeling," in *Proc. Int. Waveform Diversity Des. (WDD) Conf.*, Niagara Falls, Canada, Aug. 2010, pp. 23–27.

[27] N. H. Lehmann, A. Haimovich, R. Blum, and L. Cimini, "High resolution capabilities of MIMO radar," in *Proc. 40th Asilomar Conf. Signals, Syst., Comput.*, Pacific Grove, CA, USA, Nov. 2006, pp. 25–30.

[28] M. Akcakaya and A. Nehorai, "MIMO radar detection and adaptive design under a phase synchronization mismatch," *IEEE Trans. Signal Process.*, vol. 58, pp. 4994–5005, Oct. 2010.

[29] A. Fletcher and F. Robey, "11th conf. adaptive sensors array processing," presented at the 3rd Eur. Radar Conf., Lexington, MA, USA, Mar. 2003.

[30] I. Papoutsis, C. Baker, and H. Griffiths, "Fundamental performance limitations of radar networks," presented at the 1st EMRS DTC Tech. Conf., Edinburgh, U.K., 2004.

[31] S. Gogineni, M. Rangaswamy, B. Rigling, and A. Nehorai, "Cramer-rao bounds for UMTS-based passive multistatic radar," *IEEE Trans. Signal Process.*, vol. 62, pp. 95–106, Jan. 2014.

Sandeep Gogineni (S'08–M'14) is a Research Engineer at Wright State Research Institute in Dayton, OH. He received the B. Tech degree in electronics and communications engineering (with Honors in signal processing and communications) from International Institute of Information Technology, Hyderabad, India in 2007. He received the M.S. degree and Ph.D. degree in electrical engineering from Washington University in St. Louis, MO in 2009 and 2012, respectively. He won the Best Paper Award (First Prize) in the Student Paper Competition at the *2012 International Waveform Diversity and Design (WDD) Conference*. Further, he was selected as a Finalist in the Student Paper Competitions at *2010 International Waveform Diversity and Design (WDD) Conference* and *2011 IEEE Digital Signal Processing and Signal Processing Education Workshop*. His research interests are in statistical signal processing, radar and communications systems.

Muralidhar Rangaswamy (S'89–M'93–SM'98–F'06) received the B.E. degree in Electronics Engineering from Bangalore University, Bangalore, India in 1985 and the M.S. and Ph.D. degrees in Electrical Engineering from Syracuse University, Syracuse, NY, in 1992. He is presently employed as the Senior Advisor for Radar Research at the RF Exploitation Branch within the Sensors Directorate of the Air Force Research Laboratory (AFRL). Prior to this he has held industrial and academic appointments.

His research interests include radar signal processing, spectrum estimation, modeling non-Gaussian interference phenomena, and statistical communication theory. He has co-authored more than 150 refereed journal and conference record papers in the areas of his research interests. Additionally, he is a contributor to 8 books and is a co-inventor on 3 U.S. patents.

Dr. Rangaswamy is the Technical Editor (Associate Editor-in-Chief) for Radar Systems in the IEEE TRANSACTIONS ON AEROSPACE AND ELECTRONIC SYSTEMS (IEEE-TAES). He served as the Co-Editor-in-Chief for the *Digital Signal Processing* journal between 2005 and 2011. Dr. Rangaswamy serves on the Senior Editorial Board of the IEEE JOURNAL OF SELECTED TOPICS IN SIGNAL PROCESSING (Jan 2012–Dec 2014). He was a 2 term elected member of the sensor array and multichannel processing technical committee (SAM-TC) of the IEEE Signal Processing Society between January 2005 and December 2010 and serves as a member of the Radar Systems Panel (RSP) in the IEEE-AES Society. He was the General Chairman for the *4th IEEE Workshop on Sensor Array and Multichannel Processing (SAM-2006)*, Waltham, MA, July 2006. Dr. Rangaswamy has served on the Technical Committee of the *IEEE Radar Conference series* in a myriad of roles (Track Chair, Session Chair, Special Session Organizer and Chair, Paper Selection Committee Member, Tutorial Lecturer). He served as the Publicity Chair for the First *IEEE International Conference on Waveform Diversity and Design*, Edinburgh, U.K. November 2004. He presently serves on the conference sub-committee of the RSP. He is the Technical Program Chairman for the *2014 IEEE Radar Conference*.

He received the 2012 IEEE Warren White Radar Award, the 2013 Affiliate Societies Council Dayton (ASC-D) Outstanding Scientist and Engineer Award, the 2007 IEEE Region 1 Award, the 2006 IEEE Boston Section Distinguished Member Award, and the 2005 IEEE-AESS Fred Nathanson memorial outstanding young radar engineer award. He was elected as a Fellow of the IEEE in January 2006 with the citation for contributions to mathematical techniques for radar space-time adaptive processing. He received the 2012 and 2005 Charles Ryan basic research award from the Sensors Directorate of AFRL, in addition to more than 40 scientific achievement awards.

Brian D. Rigling (S'00–M'03–SM'08) received the B.S. degree in physics-computer science from the University of Dayton in 1998 and received the M.S. and Ph.D. degrees in electrical engineering from The Ohio State University in 2000 and 2003, respectively.

From 2000 to 2004 he was a radar systems engineer for Northrop Grumman Electronic Systems in Baltimore, Maryland. Since July 2004, Dr. Rigling has been with the Department of Electrical Engineering, Wright State University, and was promoted to associate professor in 2009 and professor in 2013. For 2010, he was employed at Science Applications International Corporation as a Chief Scientist while on leave from Wright State University.

Dr. Rigling has served on the IEEE Radar Systems Panel since 2009, and has been an associate editor for IEEE TRANSACTIONS ON IMAGE PROCESSING. He is the General Chair for the *2014 IEEE Radar Conference*.

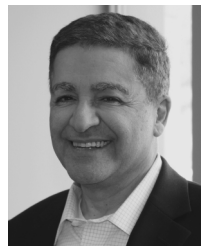

Arye Nehorai (S'80–M'83–SM'90–F'94) is the Eugene and Martha Lohman Professor and Chair of the Preston M. Green Department of Electrical and Systems Engineering (ESE) and a Professor in the Department of Biomedical Engineering at Washington University in St. Louis (WUSTL). He is also Professor in the Division of Biology and Biomedical Studies (DBBS) and Director of the Center for Sensor Signal and Information Processing at WUSTL. Earlier, he was a faculty member at Yale University and the University of Illinois at Chicago. He received the B.Sc. and M.Sc. degrees from the Technion, Israel and the Ph.D. from Stanford University, California. Under his leadership as department chair, the undergraduate enrollment has more than tripled in the last four years.

Dr. Nehorai served as Editor-in-Chief of the IEEE TRANSACTIONS ON SIGNAL PROCESSING from 2000 to 2002. From 2003 to 2005 he was the Vice President (Publications) of the IEEE Signal Processing Society (SPS), the Chair of the Publications Board, and a member of the Executive Committee of this Society. He was the founding editor of the special columns on Leadership Reflections in *IEEE Signal Processing Magazine* from 2003 to 2006.

Dr. Nehorai received the 2006 IEEE SPS Technical Achievement Award and the 2010 IEEE SPS Meritorious Service Award. He was elected Distinguished Lecturer of the IEEE SPS for a term lasting from 2004 to 2005. He received best paper awards in IEEE journals and conferences. In 2001 he was named University Scholar of the University of Illinois. Dr. Nehorai was the Principal Investigator of the Multidisciplinary University Research Initiative (MURI) project titled Adaptive Waveform Diversity for Full Spectral Dominance from 2005 to 2010. He is a Fellow of the IEEE since 1994, Fellow of the Royal Statistical Society since 1996, and Fellow of AAAS since 2012.